Effect of Pore Size of Activated Carbons Produced from Different Wood Waste on the Leakage of Phase Change Material-based Composites

Ahmet Can ,[a,b] Mehmet Emin Ergün ,[c,]* Osman Gencel ,[d] and Hikmet Yazıcı ,[e]

A shape-stabilized lauric acid-activated carbon composite was prepared using a one-step impregnation method. Activated carbon (AC) was produced from different wood waste (Scots pine (Pi) and poplar (Pop)), and lauric acid (LA) was used as a phase change material (PCM) for thermal energy storage. Wood waste from Scots pine and poplar was activated with phosphoric acid (A) and zinc chloride (S) at 600 °C for 90 min to produce AC. The AC was examined by Brunauer–Emmett–Teller (BET) analysis, and the properties of the LA/AC composites were investigated by Fourier transformation infrared spectroscope (FTIR), X-ray diffractometer (XRD), scanning electronic microscope (SEM), differential scanning calorimetry (DSC), thermal gravimetric analysis (TG), and thermal conductivity. The BET surface area of the produced AC was 1050, 1130, 625 m^2/g, and 746 m^2/g for PiA, PiS, PopA, PopS, respectively. The porous structure of AC reduced the leaching of LA during phase change. Differential scanning calorimetry (DSC) results showed a latent heat capacity of 29 J/g and a melting temperature of 48.9 °C for the LA/AC composite. The DSC results indicated that the composites exhibited the same phase change characteristics as those of the LA and their latent heats decreased. The TG results indicated that the AC could improve the thermal stability of the composites. Thermal conductivity decreased by 7.48% in PiA-PCM samples but increased by 6.86% in the PopS-PCM by AC.

DOI: 10.15376/biores.20.3.5914-5931

Keywords: Activated carbon; Phase change material; Wood waste; Lauric acid; Smart energy

*Contact information: a: Department of Forest Industry Engineering, Bartin University, 74100 Bartın, Turkey; b: Bartin University, Forest Products Application and Research Center, 74100 Bartin, Turkey, Turkey; c: Department of Forestry, Akseki Vocational School Alanya Alaaddin Keykubat University, 07630; Antalya, Turkey; d: Civil Engineering Department, Bartin University, 74100 Bartın, Turkey; e: Interior Design Program, Çaycuma Vocational School, Zonguldak Bülent Ecevit University, 67900 Çaycuma, Turkey; *Corresponding author: mehmet.ergun@alanya.edu.tr*

INTRODUCTION

Energy demand is increasing as a result of population growth and technological advancement. Around 40% of energy is used by buildings, and for people to be thermally comfortable, their living areas must be heated or cooled (Can *et al*. 2023). Insulation materials in buildings reduce energy use by lowering the need for ventilation, heating, and cooling systems, which also decreases the dependence on natural resources for energy generation. Energy storage systems are essential to ensure longer-lasting thermal comfort with less energy consumption. Phase change materials (PCMs) are substances that can store and release large amounts of thermal energy during phase transitions, usually between solid and liquid states (Socaciu 2012). PCMs can be used for thermal energy storage and thermal management applications, such as solar power harvesting, building cooling and heating, and electronic device cooling (Hekimoğlu and Sarı 2022). The PCMs can be classified into organic and inorganic types, based on their chemical composition and properties (Can 2023). However, one of the challenges of using PCMs is that they tend to leak or deform when they melt, which reduces their efficiency and durability (Chen *et al.* 2012). To overcome this problem, researchers have proposed to encapsulate PCMs in porous materials, such as activated carbons (Hussain *et al.* 2017).

Activated carbons (ACs) are porous materials that can adsorb various substances from gas or liquid phases. They are widely used for applications such as water purification, air filtration, energy storage, and catalysis (Khadiran *et al.* 2015; Chen *et al.* 2022; Ergun and Ergun 2024). The ACs can be produced from different raw materials, such as coal, wood, coconut shells, or biomass, by physical or chemical activation processes. The pore size and structure of ACs depend on the type and source of the raw material, as well as the activation method and conditions (González-García 2018; Koyuncu *et al.* 2022).

Activated carbons are carbon-based materials that have a large surface area and many pores of different sizes, which implies that they can adsorb or hold various substances (Bülbül and Ergün 2024). By filling the pores of ACs with PCMs, the leakage and deformation of PCMs can be prevented or minimized. However, the pore size of ACs may affect the performance of the PCM-AC composites. For example, the pore size may influence the amount of PCM that can be loaded, the heat transfer rate, the thermal conductivity, and the stability of the composites. Therefore, it is important to study the effect of the pore size of ACs produced from different raw materials on the leaking properties of the PCMs, as this may help to optimize the design and fabrication of PCM-AC composites for thermal energy storage applications (Li *et al.* 2020). Thermal conductivity and energy storage density were significantly enhanced by PCMs supplemented with activated carbon derived from apricot kernel shells (Hekimoğlu *et al.* 2022). In the study utilizing carbonized abandoned rice (CAR) and palmitic-lauric acid (PA-LA) eutectic mixtures, CAR was utilized as a supporting material by vacuum impregnation. Because CAR is very porous, it may act as a stabilizing matrix more easily by enhancing heat transmission and minimizing leakage. The findings showed a significant improvement, with the PA-LA/CAR composite's thermal conductivity being 1.83 times higher than that of pure PA-LA (0.44 W/mK). Furthermore, the composite exhibited notably faster rates of heat storage and release, making it suitable for practical thermal energy storage applications (Hekimoğlu *et al.* 2022). Seepage-free PCMs were created by combining carbonized kapok fiber with sugar alcohols (erythritol and mannitol). Because of its porous nature, carbonized kapok fiber offered a high loading capacity (93%) both within and outside of organic PCMs. According to An *et al.* (2019), this construction decreased the supercooling issue and boosted thermal conductivity by 130%. Yang *et al.* (2019) produced a wood-based composite PCM by impregnating TD into carbonized wood. It was discovered that the composite PCM has good thermal properties and high thermal conductivity.

In many studies involving the impregnation of phase change materials (PCMs) into activated carbon (AC), the actual contribution of AC is often misrepresented due to the presence of excess PCMs that remain on the external surface without penetrating the pores (Chen *et al.* 2012; Yuan *et al.* 2016; Ergun and Ergun 2024). These non-infiltrated PCMs can significantly influence key performance indicators such as leakage rate and latent heat, leading to inaccurate assessments of AC's true effectiveness. To address this issue, it is essential to remove the surplus PCM through a washing process. This step ensures that only the PCM retained within the porous structure of AC is evaluated, allowing for a more accurate determination of the material's impact on thermal performance.

Sustainable utilization of natural resources and reduction of environmental impacts are among the foremost priorities of our era. Therefore, the control and recycling of waste generated in energy production and industrial processes are crucial steps in achieving environmental sustainability. So, the production of AC emerges as an effective strategy for the economic and ecological valorization of organic waste. This study examined how ACs are produced from white poplar (*Populus alba*) and Scots pine (*Pinus sylvestris*) wood waste, using phosphoric acid (H_3PO_4) and zinc chloride ($ZnCl_2$). The goal was to overcome leaking properties by incorporating a PCM.

EXPERIMENTAL

Materials

The white poplar (*Populus alba*) and Scots pine (*Pinus sylvestris*) wood residues used in this study were obtained in the form of powder and free of charge from an enterprise in Bartın. Zinc chloride ($ZnCl_2$) and phosphoric acid (H_3PO_4) were used in the activation process, while hydrochloric acid (HCl) and potassium hydroxide (KOH) were used during the washing of the produced ACs. $ZnCl_2$, H_3PO_4, HCl, and KOH were of analytical purity, and they were obtained from Merk (Darmstadt, Germany) or Fluka (Jul, Switzerland) companies. In this study, AC production was carried out using black poplar and pine wood with the help of acid (phosphoric acid) and salt (zinc chloride) activation agents.

Activated Carbon Production

Activated carbon was produced separately from two types of biomass—Scots pine (*Pinus sylvestris*) and white poplar (*Populus alba*)—using two chemical activation methods: phosphoric acid (AC-A) and zinc chloride (AC-S) following procedures described in previous studies (Liou 2010; Heidarinejad *et al.* 2020; Ergun *et al.* 2025). For each wood type, 500 g of precursor material was individually mixed with 500 mL of 50% phosphoric acid and 500 mL of water (for AC-A), or with 250 g of $ZnCl_2$ and 725 mL of water (for AC-S). The mixture was dried at 70 °C for 24 h after being heated to 110 °C for 2 h in order to activate the acid. The material was kept at room temperature for 24 h before drying in order to activate the salt. The dried precursors were activated in in a tubular furnace (Henan Sante Furnace Technology Co. Ltd, model STG-40-14, Henan, China) under a continuous nitrogen flow of 50 mL/min at 600 °C for 1.5 h. After cooling, the acid-activated samples were first washed with 0.5 M KOH solution and then thoroughly rinsed with hot water until the pH reached a neutral value (6.5 to 7). All activated carbons were then dried at 90 °C for 6 h and ground into fine powder. The AC samples were named as PiA and PiS for pine-derived samples, and PopA and PopS for poplar-derived samples.

Synthesis of Shape-Stabilized LA/AC Composites

The activated carbon (AC) was dried for 12 h at 110 °C in an oven to remove any remaining moisture. Lauryl alcohol (LA) was first heated above its melting point (43 to 45 °C) and subsequently dissolved in 25 mL of acetone to prepare a homogeneous solution. The lauryl alcohol (LA) mixture was maintained at 45 ± 2 °C during the impregnation process to ensure that it remained in the liquid phase and could effectively diffuse into the pores of the activated carbon. The melted LA solution was then mixed with the pre-dried AC at a ratio of X:1 (LA:AC, w/w) and stirred at 400 rpm for 4 h at ambient conditions to allow for the infiltration of LA into the AC pores. The resulting slurry was dried in an oven at 80 °C for 24 h to ensure complete evaporation of the acetone and to obtain the shape-stabilized LA/AC composites. No vacuum treatment was applied during impregnation; the process relied solely on mechanical stirring and solvent-assisted diffusion.

To determine the amount of PCM successfully impregnated into the AC, each sample was weighed before and after the impregnation-drying process using a precision balance (±0.1 mg accuracy). The weight increase due to LA loading was calculated using Eq. 1,

$$\text{PCM loading (\%)} = (W_{\text{final}}-W_{\text{initial}})/W_{\text{initial}})\text{X}100 \tag{1}$$

where W_{initial} is the weight of the dry AC and W_{final} is the weight after impregnation and drying. All samples were stored in a desiccator before and after the process to minimize moisture interference. The resulting composites, as shown in Fig. 1, are referred to as PiA-PCM, PiS-PCM, PopA-PCM, and PopS-PCM based on the type of AC and source material used.

Characterization of AC and LA/AC Composites

Using a Quantachrome autosorb IQ BET device (Quantachrome Corporation, Graz, Austria), nitrogen gas adsorption/desorption isotherm measurements were used to identify structural characteristics such as the the BET surface area. Micropore volume analyses were performed only on the activated carbon samples prior to lauric acid impregnation, as degassing at 120 °C for 3 h. The chemical structures of PiA, PiS, PopA, PopS, and LA/AC composites were determined by Fourier transformation infrared spectrometer (FTIR, LB-119, Labser, Istanbul, Turkey) in spectra range from 4000 to 400 cm^{-1} using KBr pellets. All LA/AC composites samples and AC were treated by gold spraying under vacuum to observe their micro-structure by scanning electron microscope (SEM, Maıa3 Xmu, Tescan, Brno, Czech Republic). The crystalline phase of LA/AC composites, and AC were analyzed by X-ray diffractometer (XRD, Panalytical, Empyrean, Malvern, United Kingdom) within angle range of 10° to 60° with a speed of 2θ (5°/min). The enthalpy and melting-solidifying temperature of the LA/AC composites were analyzed by differential scanning calorimetry (DSC, Hitachi, DSC7020, Hitachinaka, Japan) within the temperature range of 20 to 60 °C at the temperature change of 5 °C/min under a continuous nitrogen flow. The residual weight of the LA/AC composites and AC was tested by thermogravimetric analysis (TGA Hitachi -STA 7300, Hitachinaka, Japan) at room temperature to 700 °C under the condition of continuous nitrogen flow and a heating rise of 20 °C/min. Thermal conductivity value of AC and LA/AC composites were measured with precision of ±4% using a thermal conductivity analyzer (Linseis, THB Advance model Transient Hot Bridge Analyzer).

RESULTS AND DISCUSSION

Physical Properties of AC

The results showed the characteristics of AC produced from two types of sawmill residues, Scots pine (Pi) and white poplar (Pop), by two different chemical activation methods, based on phosphoric acid (H_3PO_4) and zinc chloride ($ZnCl_2$), respectively. The main parameters that were measured were the surface area, the pore volume, the pore diameter, and the yield of the AC samples (Table 1).

Table 1. Physical Properties of AC

	Surface Area (m^2/g)	V_{micro} (cm^3/g)	V_{mezo} (cm^3/g)	V_{total} (cm^3/g)	D_p (nm)	Yield (%)	PCM Loading (%)
PiA	1053.11	0.415	0.183	0.598	1.62	31.27	54.90
PiS	1126.45	0.443	0.076	0.519	1.55	32.43	30.00
PopA	625.46	0.210	0.199	0.409	1.43	32.77	53.00
PopS	746.38	0.275	0.089	0.364	1.35	31.68	19.00

V_{micro}: Micro-pore volume, V_{mezo}: Mesopore volume, V_{total}: Total pore volume, D_p: Average pore diameter

The surface area of the AC samples is an important indicator of their adsorption capacity, as it reflects the availability of active sites for the interaction with adsorbate molecules. While surface area is often used as a general indicator of adsorption capacity, it is the pore structure parameters—such as pore size and volume—that are of greater relevance in this context. Since the lauric acid must undergo melting and solidification to function as a phase change material, it must be absorbed in bulk within the porous matrix via capillary action, rather than forming only a surface monolayer. Therefore, adequate pore size and volume are essential to accommodate sufficient amounts of PCM and allow for phase transition behavior. The AC samples produced by $ZnCl_2$ activation have higher surface area than those produced by H_3PO_4 activation, regardless of the type of biomass. $ZnCl_2$ is a more effective activating agent than H_3PO_4, as it can create more micropores and mesopores in the carbon structure (Heidarinejad *et al.* 2020). Among the four AC samples, the highest surface area was obtained for the AC from Scots pine waste using $ZnCl_2$ activation, with a value of 1130 m^2/g. Scots pine residue is a suitable precursor for AC production, as it has a high carbon content (Serafin and Dziejarski 2024). It is thought that the reason why the surface area of the AC obtained from the coniferous Scots pine waste was higher than that of the broad-leaved poplar waste is not only related to the higher carbon content. Several factors can account for the effective production from Scots pine residues. First of all, coniferous tree species such as Scots pine have higher lignin and resin contents and a denser cellular structure. In addition, the high lignin content of Scots pine not only enhances the interaction with $ZnCl_2$ during activation, promoting micropore formation, but it also contributes to the development of a highly aromatic and thermally stable biochar structure, which is favorable for activated carbon production (Sun *et al.* 2023). On the other hand, the cellular structure allows the formation of a wider micropore network under chemical activation conditions and as a result, provides a higher surface area. In addition, the $ZnCl_2$ activation method promotes the development of micropores and the high lignin content of Scots pine interacts more effectively with $ZnCl_2$, providing a porous structure. The high lignin and carbon contents also increases the thermal stability of Scots pine, allowing it to withstand higher activation temperatures, which contributes to the higher surface area.

The pore volume and the pore diameter of the AC samples are also related to their adsorption performance, as they determine the accessibility and the size distribution of the pores. The AC samples produced by H_3PO_4 activation had higher total pore volume and mesopore volume than those produced by $ZnCl_2$ activation, while the opposite is true for the micropore volume. This implies that H_3PO_4 activation tends to create more mesopores, while $ZnCl_2$ activation tends to create more micropores in the carbon matrix (Liou 2010). The pore diameter of the AC samples is inversely proportional to their surface area, as expected from the BET theory. The smallest pore diameter was observed for the AC from white poplar waste by $ZnCl_2$ activation, with a value of 1.35 nm. This AC sample had a high proportion of micropores, which are favorable for the adsorption of small molecules (Ahmad *et al.* 2021).

The yield of the AC samples is an economic factor that reflects the efficiency of the AC production process. The results show that the AC samples produced by H_3PO_4 activation had higher yield than those produced by $ZnCl_2$ activation, regardless of the type of biomass. This result is similar with the literature, which reports that H_3PO_4 activation has a lower carbon loss than $ZnCl_2$ activation, as the former is a milder and less corrosive agent than the latter (Yahya *et al.* 2015; Gao *et al.* 2020). Among the four AC samples, the highest yield was obtained for the AC from white poplar waste by H_3PO_4 activation, with a value of 32.8%.

The results demonstrated that both Scots pine waste and white poplar waste can be used as precursors for AC production by chemical activation with H_3PO_4 or $ZnCl_2$. The choice of the activating agent and the type of biomass affects the characteristics of the AC samples, such as the surface area, the pore volume, the pore diameter, and the yield. The AC samples produced by $ZnCl_2$ activation had higher surface area and micropore volume, while the AC samples produced by H_3PO_4 activation had higher total pore volume and mesopore volume. The AC samples from Scots pine waste had higher surface area and smaller pore diameter than the AC samples from white poplar waste. The AC samples from white poplar waste had higher yield than the AC samples from Scots pine waste.

Leakage Testing of PCM

Leakage testing of AC composite form-stable PCMs is crucial to solving the PCM leakage problems in building materials. Figure 1 shows images from the leakage tests of the AC composite form-stable PCMs. The samples of AC composite form-stable PCMs were poured onto the paper surface, as shown in Fig. 1. Every sample was put on a heating stage where the temperature was raised from 45 to 60 °C for a period of 30 to 60 min. It was observed that there was no leakage in the samples at 45 °C for 30 min. Leaching was observed in PiA, PiS, and PopA samples of AC composite materials kept at 60 °C for 30 min; however, no leaching was observed under those conditions in the case of PopS samples. The green lines in the Fig. 1 show the extends of leaching at 30 min. The extent of leaching increased with the passage of time at 60 degrees, and the lowest leaching (red line) was obtained in PopS samples at the end of 60 min. Although the PopS samples gained 53% weight gain after impregnation with PCM, the low leaching can be attributed to the physical properties of the PopS samples in Table 1.

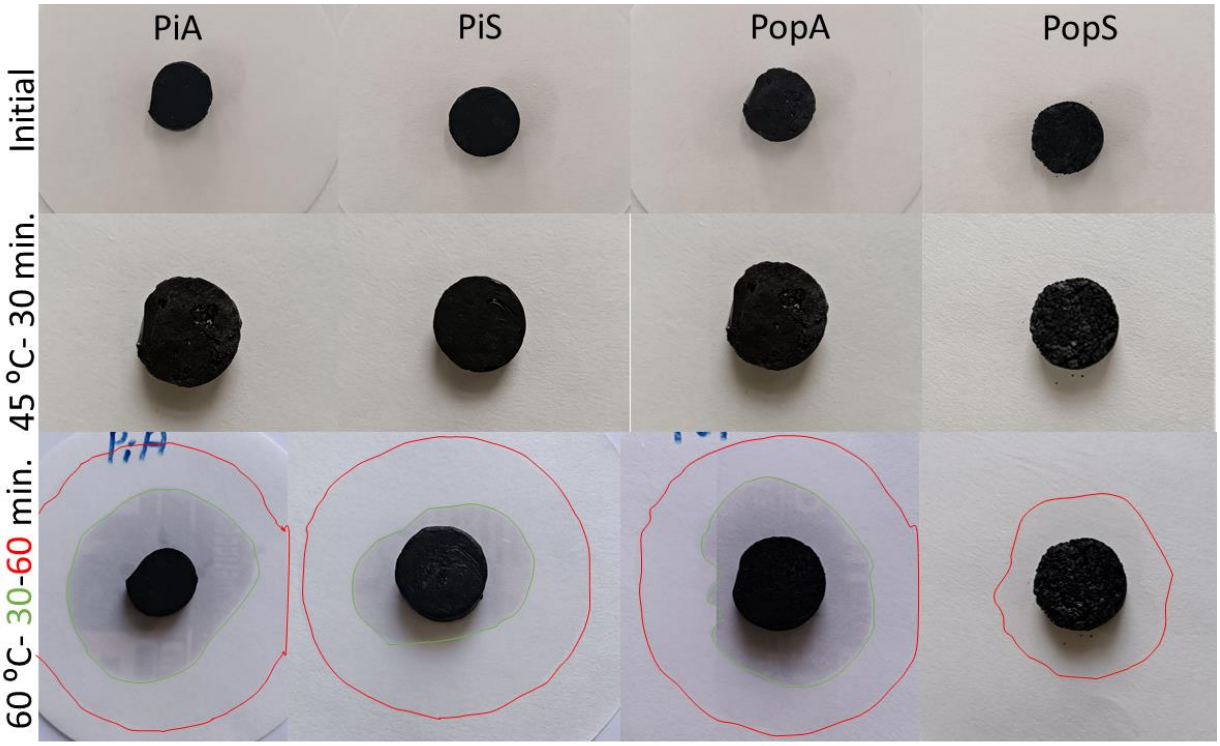

Fig. 1. Photographs of leakage tests of AC composite

Micromorphology Analysis of the AC and Lauric Acid/AC Composites

The SEM images of the PCM-filled ACs and the AC are shown in Figs. 2 and 3. The white particles in the images stand in for the LA. Four distinct ACs are shown to have varying pore diameters. Because the AC has numerous pores with several interior surfaces, as seen in Figs. 2 and 3, it can be readily saturated with the melted LA. Because of the surface tension and capillary forces between the LA and the AC's porous network, the LA became distributed uniformly in the composites. The AC’s porous structure kept the melted LA from seeping through and gave the composite sand a respectable mechanical strength overall. Despite the 53% WPG ratio, the leaching in PopS samples remained low, which was attributed to their narrow pore diameter. Stated differently, it appears that the leaching of PCM is influenced by the pore diameter of AC.

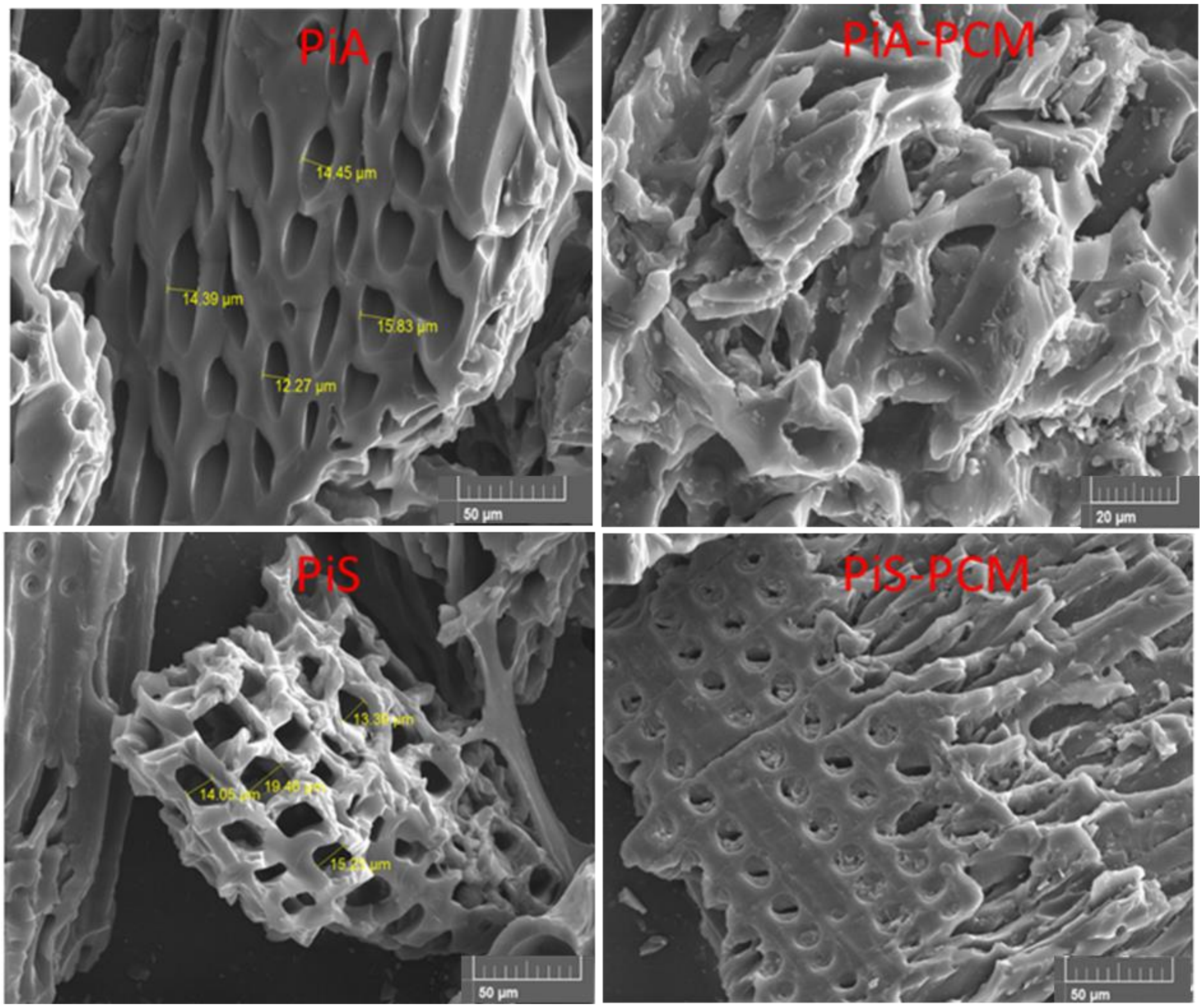

Fig. 2. SEM photographs of the ACs (PiA, PiS) obtained from pine wood and lauric acid/AC composites (PiA-PCM, PiS-PCM)

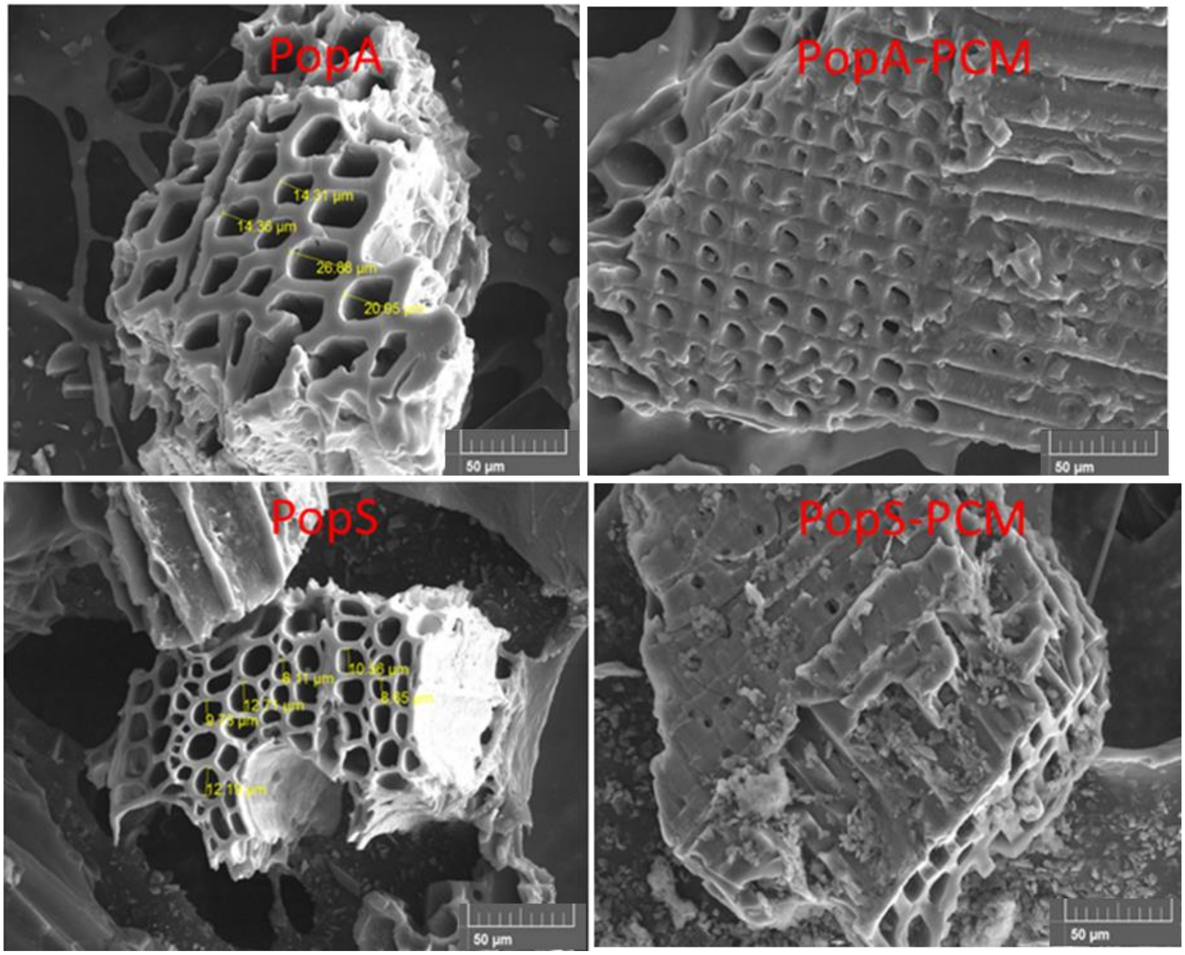

Fig. 3. SEM photographs of the ACs (PopA, PopS) obtained from poplar wood and lauric acid/AC composites (PopA-PCM, PopS-PCM)

Chemical Structure Analysis by FTIR Spectrum

The FTIR spectra of the PopS and PopS-PCM are shown in Fig. 4. The symmetrical stretching vibration of the $–CH_3$ group is represented by the peaks of LA at 2917 cm^{-1}, while the symmetrical stretching vibration of the $–CH_2$ group is represented by the peak at 2849 cm^{-1} (Chen *et al*. 2012). The stretching vibration of C–O is responsible for the peak at 1701 cm^{-1}. The in-plane bending vibration and out-of-plane bending vibration of the –OH functional group in LA are represented by peaks at 1303 and 938 cm^{-1}, respectively. The OH functional group's in-plane swinging vibration is represented by the peak at 721 cm^{-1} (Chen *et al.* 2012).

The LA absorbance and the AC bands at 1510 cm^{-1} were present in the FTIR spectra of PopS-PCM. Additionally, the peak originating from AC at 1560 cm^{-1} was observed in PopS-PCM samples. These findings suggest that the interaction between LA and AC during the composite preparation is primarily physical in nature, as no obvious new peaks were observed in the FTIR spectra. Physical absorption allows for the absorption of LA by surface tension and capillary forces inside the porous network of the AC. This partially prevents the melted LA from leaking out of the composites. The preservation of characteristic LA absorbance bands in the FTIR spectrum indicates good chemical stability after impregnation, which is consistent with previous findings that attribute such stabilization to the structural support provided by activated carbon (Wang *et al.* 2012).

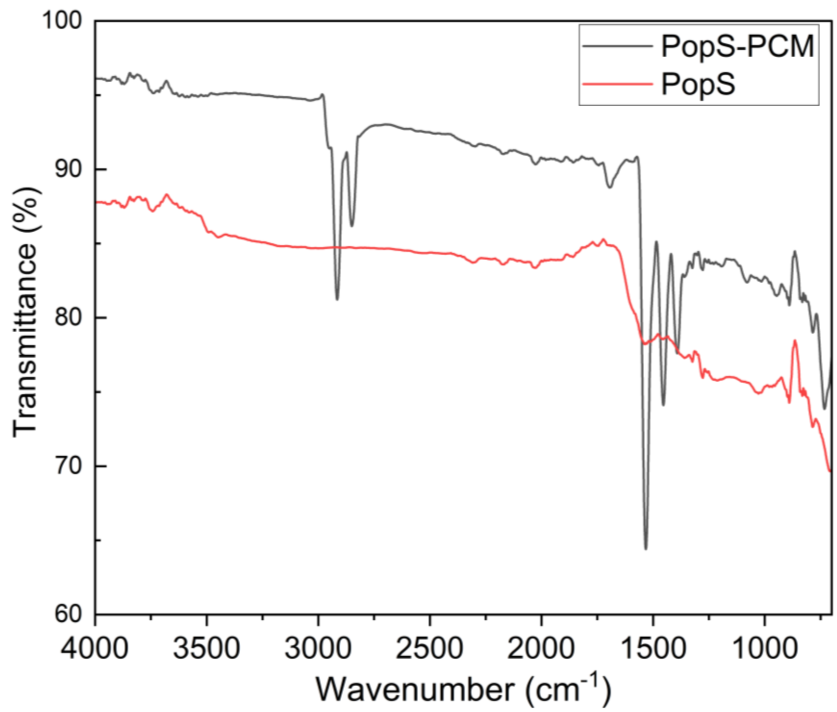

Fig. 4. FTIR spectra of PopS and PopS-PCM

Analysis of AC and Lauric Acid/AC Composites by XRD Patterns

Fig. 5 displays the XRD patterns of the PopS and PopS-PCM. The flat apex of the AC may be seen at approximately 24.81° in Fig. 5. This finding suggests that the AC has an amorphous porous structure and is not crystalline. In the literature, the XRD peaks at 18.71°, 20.41°, 21.71°, 24.11°, 26.51°, and 40.51° have been attributed to the LA due to its regular crystallization (Chen *et al.* 2012). Figure 5 shows that the flat peak of AC serves as the foundation for the presentation of the PopS-PCM in the XRD patterns of the composites. This outcome suggests that there is no clear evidence of changes in the crystalline structure of LA within the AC matrix during the synthesis process. Furthermore, the strength of PopS-PCM peaks was lower than that of LA crystal peaks reported in the literature. This finding suggests that the LA’s crystals were constrained by the AC's pores, causing the LA's crystallite size to decrease in the composites.

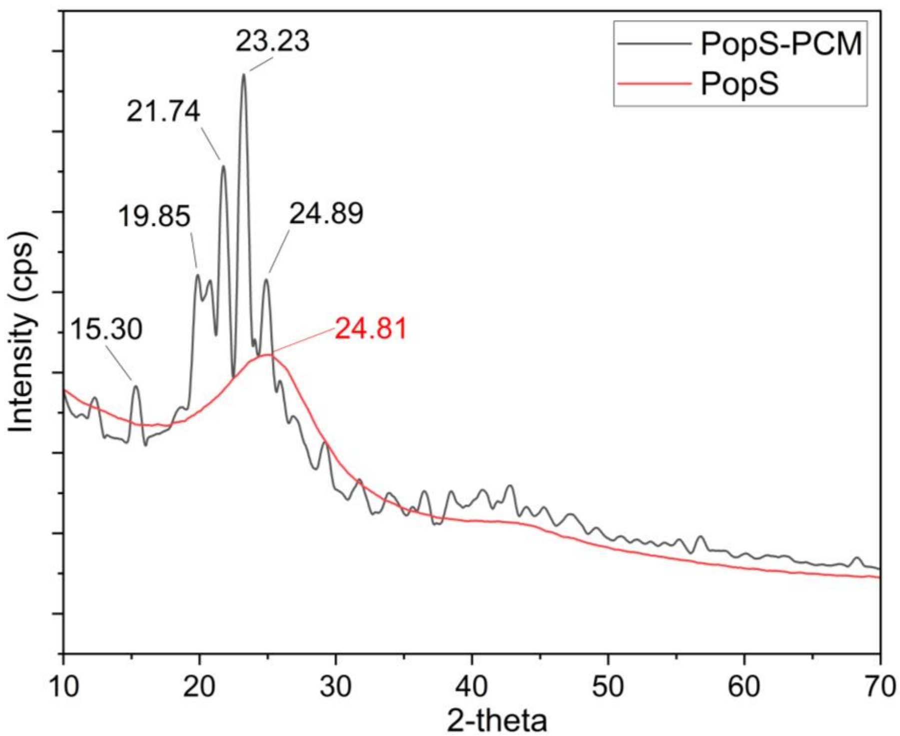

Fig. 5. XRD patterns of the PopS and PopS-PCM

The DSC Analysis of Lauric Acid/AC Composites

The DSC results of the lauric acid/AC composites are shown in Figs. 6 and 7, which show the latent heat of LA/AC composites. In the two figures, the melting and solidifying temperatures were determined to be 44.3 and 38.9 °C for the LA, respectively, and 43.9 and 40.0 °C for the PiA-PCM, 43.7 and 39.7 °C for the PiS-PCM, 44.0 and 39.7 °C for the PopA-PCM, and 43.3 and 40.3 °C for the PopS-PCM. The melting and solidifying latent heats were measured to be 208.1 and 207.8 J/g for the LA, respectively, 29.4 and 28.9 J/g for the PiA-PCM, 24.1 and 22.4 J/g for the PiS-PCM, 27.7 and 26.4 J/g for the PopA-PCM, and 26.9 and 25.8 J/g for the PopS-PCM. This temperature range is highly relevant for low-temperature thermal energy storage applications, such as passive heating in buildings, especially for maintaining indoor thermal comfort during moderate climate conditions. Additionally, it is suitable for solar thermal systems and temperature-sensitive packaging materials.

A high PCM content will result in a high latent heat storage capacity, since only the PCM in composites absorbs and releases thermal energy during the melting and solidification process. As a result, PiA-PCM was selected as a promising material for thermal energy storage. It was found that the greatest mass percentage of LA in the composites was 54.9%.

The melting and solidification temperatures of LA, PiA-PCM, PiS-PCM, PopA-PCM, and PopS-PCM differed by 5.5, 3.9, 4.0, 4.4, and 3.0 °C, respectively, as illustrated in Fig. 6. This finding suggests that because AC acts as a nucleation agent and has a porous wall, the LA/AC composites supercool to a lower degree during solidification in comparison to ordinary LA. In addition, the fact that the lowest difference was obtained in PopS-PCM samples with smaller pore sizes supports this situation and similar results are also obtained in XRD results (Fig. 5).

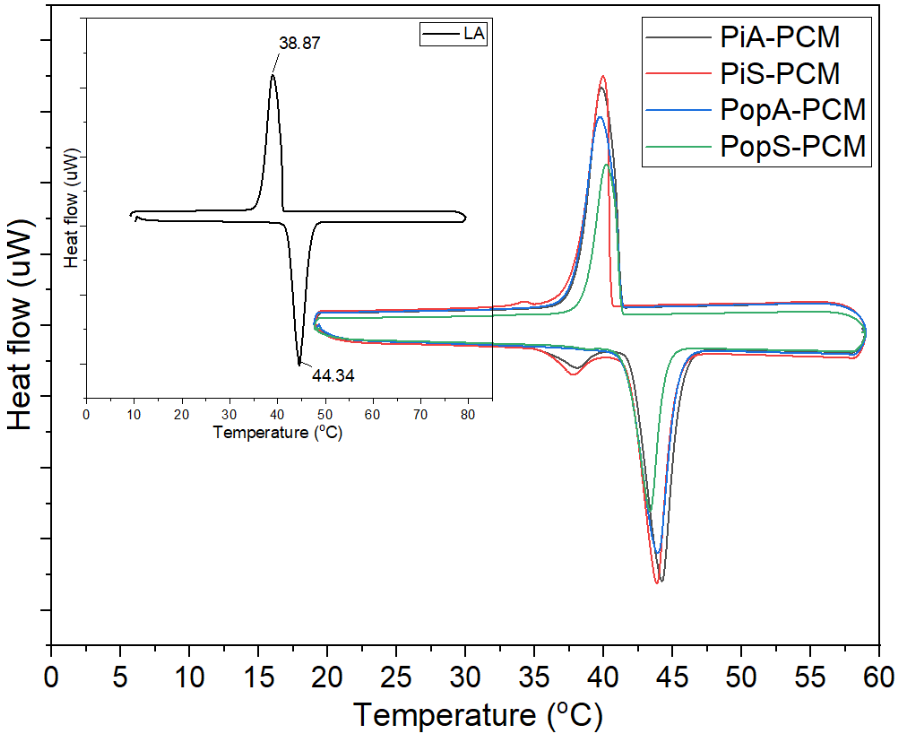

Fig. 6. DSC thermogram of pure LA and lauric acid/AC composites

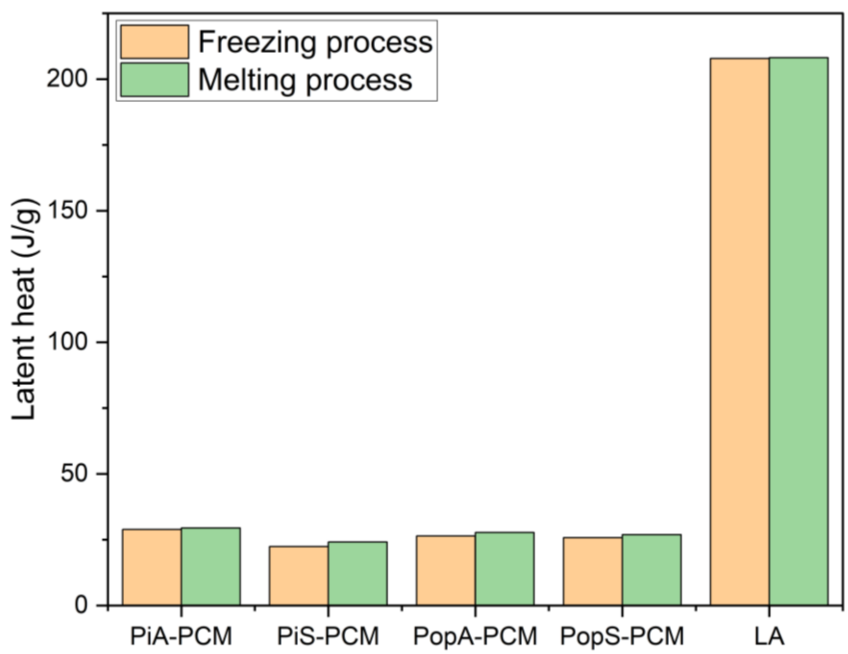

Fig. 7. Latent heats (J/g) of pure LA and lauric acid/AC composites

Table 2 lists the performance metrics, such as the mass percentage of fatty acids in the shape-stable composite phase change materials (CPCMs), melting temperature, and melting enthalpy, that were compared with earlier experimental studies employing fatty acids as an energy storage carrier. Under the same support material, it can be observed that the lauric acid/AC composites developed in this work had a good heat storage capacity.

Table 2. Comparison of this Study with Others in the Literature

AC/PCMs	Melting Temperature (°C)	Melting Enthalpy (J/g)	Reference
Lauric acid/AC	43.87	32.45	(Chen *et al.* 2012)
Lauric acid-Myristic acid/AC	38.49	35.46	(Chen *et al.* 2022)
Capric-palmitic-stearic acid/AC	19.82	34.62	(Yuan *et al.* 2016)
Octanoic-lauric acid/expanded graphite	3.6	132.8	(Li *et al.* 2019)
Beeswax/multi-walled carbon nanotubes	59.8	91.6	(Putra *et al.* 2019)
Lauric acid/PiA	43.88	29.44	Present study

TGA Results of Lauric Acid/AC Composites

The TGA and DTG curves of the LA, and LA/AC composites are shown in Figs. 8 and 9, respectively. There was a two-step process of thermal degradation, as shown in Fig. 8. During the two-step thermal degradation processes, the PopS-PCM lost more weight than the PiA-PCM, PiS-PCM, and PopA-PCM combined. This is because the LA mass in the PopS-PCM was greater than the LA mass in the PiA-PCM, PiS-PCM, and PopA-PCM. The thermal degradation of the LA molecular chains was represented by the first step, which took place at a temperature of between 20 and 150 °C, as illustrated in Fig. 8. The second phase, which is the thermal breakdown of the AC, occurred between 150 and 400 °C. According to literature studies (Zhang *et al.* 2009; Chen *et al.* 2012), although LA is completely decomposed at 600 °C, AC remains at approximately 50% at this temperature. Therefore, AC is advantageous in creating carbonaceous layers that form a physical protective barrier on the surface of composites. The similar residual weights observed in PiS and PiS-PCM samples at the end of the thermal degradation process can be attributed to the early decomposition and volatilization of the PCM at lower temperatures. Since the lauryl alcohol degraded and evaporated mostly below 250 °C, the remaining matrix was essentially the PiS structure. As a result, by the end of the test (at 700 °C), both samples behaved similarly in terms of residue, reflecting the thermal stability characteristics of the PiS framework alone. This protective barrier can limit the transition of combustible molecules to the gas phase and the heat from the flame to the condensed phase (Zhang *et al.* 2009). This result shows that the AC was able to increase the thermal stability of composites.

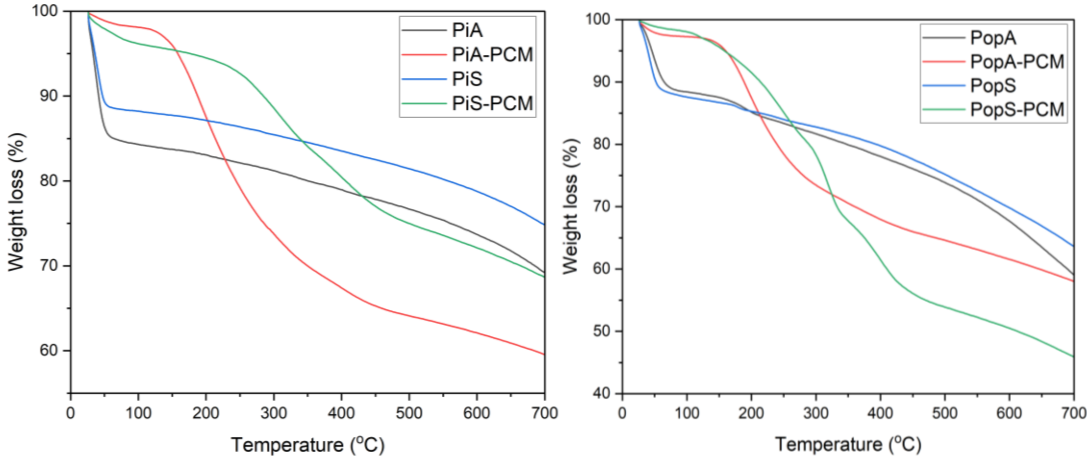

Fig. 8. TGA curves of the AC and lauric acid/AC composites

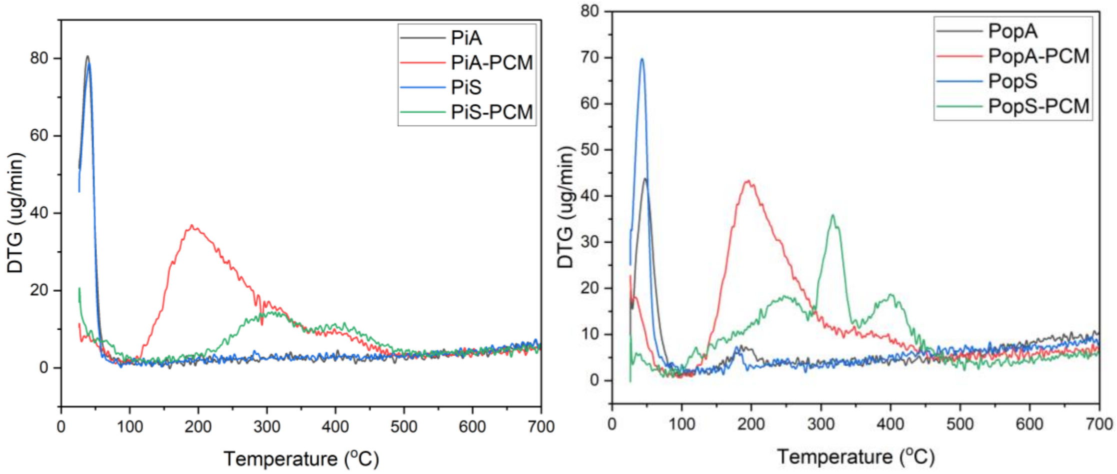

Fig. 9. DTG curves of the AC and lauric acid/AC composites

Thermal Conductivity of LA, AC, and Lauric Acid/AC Composites

Thermal conductivity of LA, AC, and LA/AC composites were measured, and the data are shown in Table 3.

Table 3. Thermal Conductivity of LA, CA, Lauric Acid/AC Composites and Different PCMs

Sample Name	Thermal Conductivity (W/(m·K))	
LA	0.112	Present study
AC	0.102	
PopA-PCM	0.105	
PopS-PCM	0.109	
PiA-PCM	0.094	
PiS-PCM	0.098	
Lauric acid/activated carbon	0.15	(Chen *et al.* 2012)
Lauric–palmitic acid/polyvinyl butyral/carbon nanofibers	0.40	(Xu *et al.* 2022)
Lauric–palmitic acid/poly(ethylene terephthalate)/Cu	0.15	(Rezaie and Montaze 2019)
Lauric –capric acid/diatomite/expanded graphite	0.46	(Wen *et al.* 2018)

The changes in thermal conductivity observed in LA/AC composites appeared to be related to the differences in the surface area and pore structure of the AC. The thermal conductivity of LA was determined as 0.112 W/(m K), while that of AC was determined as 0.102 W/(m K). The thermal conductivity values obtained in this study were measured as 0.105, 0.109, 0.094, and 0.098 W/(m K) for PopA-PCM, PopS-PCM, PiA-PCM, and PiS-PCM composites, respectively. The observed differences in thermal conductivity among the AC-based samples (PopS-PCM and PiS-PCM) appear to be primarily influenced by the amount of PCM loaded into the activated carbon matrix, rather than the pore structure resulting from $ZnCl_2$ activation. As shown in Table 1, PiS-PCM contains approximately 30% PCM and PopS-PCM has about 19%. The lower PCM content in PopS-PCM and PiS-PCM may have contributed to its relatively higher thermal conductivity. On the other hand, the decrease observed in PiA-PCM (Scots Pine, H_3PO_4) may be due to its less efficient pore structures in terms of heat conduction. The fact that the thermal conductivity values in the composites were close to the individual thermal conductivity values of LA and AC indicates that the effect of the pore structure on heat conduction was limited. However, the lower thermal conductivity values obtained compared to other studies in the literature may be due to the differences in the AC structure properties and preparation methods involved in this study.

CONCLUSIONS

In this study, shape-stabilized phase change composites were successfully developed using lauric acid and activated carbon (AC) derived from wood wastes of Scots pine and poplar. The results are summarized below:

1. Activated carbon with high specific surface areas (625 to 1126 m^2/g) was obtained *via* $ZnCl_2$ activation of wood waste, offering a sustainable valorization route for lignocellulosic biomass.

2. Lauric acid was successfully impregnated into the porous network of AC, resulting in composites with good shape stability and suppressed leakage.

3. The composites exhibited phase change behavior similar to pure lauric acid, with a melting temperature of ~48.9 °C and a latent heat of 29.4 J/g.

4. Thermogravimetric analysis (TGA) confirmed that thermal stability improved after the incorporation of AC, supporting the stabilizing effect of the carbon matrix on PCM.

5. Thermal conductivity behavior varied depending on the phase change material (PCM) loading ratio. Notably, samples with lower PCM loading (*e.g.*, PopS-PCM, 19%) showed increased conductivity, suggesting that PCM ratio can influence heat transfer more significantly than surface area alone.

6. This study provides new insight into how PCM loading ratio, rather than just AC surface area, governs thermal conductivity in shape-stabilized composites—an aspect often overlooked in the literature.

7. Furthermore, our findings indicate that biomass-derived AC can be a viable and eco-friendly carrier for PCMs, supporting future research in sustainable thermal energy storage materials.

8. The work also suggests that careful balance between porosity, PCM content, and processing conditions is essential for optimizing both latent heat capacity and thermal conductivity.

In order to better adapt the pore size distribution of activated carbon to phase change material (PCM) encapsulation, future studies might investigate other activation techniques. Although the $ZnCl_2$ activation used in this work produced a mixture of micro- and mesopores, it is well known that differing porosity profiles are advantageous for various applications. A preponderance of large mesopores may increase impregnation and retention of molten PCM while reducing leakage for thermal energy storage, particularly with organic PCMs such as lauric acid. On the other hand, too much microporosity may decrease latent heat capacity and restrict PCM accessibility. Thus, assessing the impact of various pore structures—achieved using different activation methods or precursors—may offer more profound understanding of how to optimize shape-stabilized PCM composites. The optimal pore size distribution and range for optimizing shape stability and thermal performance would be determined with the aid of such studies.

REFERENCES CITED

Ahmad, A. A., Al-Raggad, M., and Shareef, N. (2021). "Production of activated carbon derived from agricultural by-products via microwave-induced chemical activation: A review," *Carbon Letters* 31(5), 957-971. DOI: 10.1007/s42823-020-00208-z

An, J., Liang, W., Mu, P., Wang, C., Chen, T., Zhu, Z., Sun, H., and Li, A. (2019). "Novel sugar alcohol/carbonized kapok fiber composites as form-stable phase-change materials with exceptionally high latent heat for thermal energy storage," *ACS Omega* 4(3), 4848-4855. DOI: 10.1021/acsomega.8b03373

Bülbül, Ş., and Ergün, H. (2024). "Investigation of the usability of activated carbon as a filling material in nitrile butadiene rubber/natural rubber components and modeling by regression analysis," *Journal of Elastomers and Plastics* 56(1), 53-73. DOI: 10.1177/00952443231215469

Can, A. (2023). "Preparation, characterization, and thermal properties of microencapsulated palmitic acid with ethyl cellulose shell as phase change material impregnated wood," *Journal of Energy Storage* 66, article 107382. DOI: 10.1016/j.est.2023.107382

Can, A., Lee, S. H., Antov, P., and Abd Ghani, M. A. (2023). "Phase-change-material-impregnated wood for potential energy-saving building materials," *Forests* 14(3), article 514. DOI: 10.3390/f14030514

Chen, Y., Ge, M., Zhao, F., and Yang, X. (2022). "Synthesis of lauric-myristic acid/activated carbon composite as a new shape-stabilized energy storage material," *Materials Science* 28(1), 68-74. DOI: 10.5755/j02.ms.26840

Chen, Z., Shan, F., Cao, L., and Fang, G. (2012). "Synthesis and thermal properties of shape-stabilized lauric acid/activated carbon composites as phase change materials for thermal energy storage," *Solar Energy Materials and Solar Cells, Organic, Dye-Sensitized and Innovative Approaches for Photovoltaic Applications* 102, 131-136. DOI: 10.1016/j.solmat.2012.03.013

Ergun, M. E., and Ergun, H. (2024). "Influence of activated carbon concentration on foam material properties: design and optimization," *Arabian Journal for Science and Engineering* 49(4), 4877-4888. DOI: 10.1007/s13369-023-08275-w

Ergun, M. E., Koyuncu, F., Istek, A., snf Özlüsoylu, İ. (2025). "Reducing formaldehyde emissions and enhancing performance of particleboards through the incorporation of activated carbon produced from Scots pine wood residues," *Biofuels, Bioproducts and Biorefining* online first. DOI: 10.1002/bbb.2788.

Gao, Y., Yue, Q., Gao, B., and Li, A. (2020). "Insight into activated carbon from different kinds of chemical activating agents: A review," *Science of the Total Environment* 746, article 141094. DOI: 10.1016/j.scitotenv.2020.141094

González-García, P. (2018). "Activated carbon from lignocellulosics precursors: A review of the synthesis methods, characterization techniques and applications," *Renewable and Sustainable Energy Reviews* 82, 1393-1414. DOI: 10.1016/j.rser.2017.04.117

Heidarinejad, Z., Dehghani, M. H., Heidari, M., Javedan, G., Ali, I., and Sillanpää, M. (2020). "Methods for preparation and activation of activated carbon: A review," *Environmental Chemistry Letters* 18(2), 393-415. DOI: 10.1007/s10311-019-00955-0

Hekimoğlu, G., and Sarı, A. (2022). "A review on phase change materials (PCMs) for thermal energy storage implementations," *Materials Today: Proceedings, 3rd International Congress on Materials and Structural Stability* 58, 1360-1367. DOI: 10.1016/j.matpr.2022.02.231

Hussain, S. I., Dinesh, R., Roseline, A. A., Dhivya, S., and Kalaiselvam, S. (2017). "Enhanced thermal performance and study the influence of sub cooling on activated carbon dispersed eutectic PCM for cold storage applications," *Energy and Buildings* 143, 17-24.

Khadiran, T., Hussein, M. Z., Zainal, Z., and Rusli, R. (2015). "Activated carbon derived from peat soil as a framework for the preparation of shape-stabilized phase change material," *Energy* 82, 468-478. DOI: 10.1016/j.energy.2015.01.057

Koyuncu, F., Güzel, F., and İnal, İ. I. G. (2022). "High surface area and supermicro-porous activated carbon from capsicum (*Capsicum annuum* L.) industrial processing pulp via single-step KOH-catalyzed pyrolysis: Production optimization, characterization and its some water pollutants removal and supercapacitor performance," *Diamond and Related Materials* 124, article 108920. DOI: 10.1016/j.diamond.2022.108920

Li, Y., Zhang, X., Munyalo, J. M., Tian, Z., and Ji, J. (2019). "Preparation and thermophysical properties of low temperature composite phase change material octanoic-lauric acid/expanded graphite," *Journal of Molecular Liquids* 277, 577-583. DOI: 10.1016/j.molliq.2018.12.111

Li, Z., Shahsavar, A., Al-Rashed, A. A. A. A., and Talebizadehsardari, P. (2020). "Effect of porous medium and nanoparticles presences in a counter-current triple-tube composite porous/nano-PCM system," *Applied Thermal Engineering* 167, article 114777. DOI: 10.1016/j.applthermaleng.2019.114777

Liou, T. H. (2010). "Development of mesoporous structure and high adsorption capacity of biomass-based activated carbon by phosphoric acid and zinc chloride activation," *Chemical Engineering Journal* 158(2), 129-142. DOI: 10.1016/j.cej.2009.12.016

Putra, N., Rawi, S., Amin, M., Kusrini, E., Kosasih, E. A., and Indra Mahlia, T. M. (2019). "Preparation of beeswax/multi-walled carbon nanotubes as novel shape-stable nanocomposite phase-change material for thermal energy storage," *Journal of Energy Storage* 21, 32-39. DOI: 10.1016/j.est.2018.11.007

Rezaie, A. B., and Montazer, M. (2019). "*In situ* incorporation and loading of copper nanoparticles into a palmitic–lauric phase-change material on polyester fibers," *Journal of Applied Polymer Science* 136(3), article 46951. DOI: 10.1002/app.46951

Serafin, J., and Dziejarski, B. (2024). "Activated carbons—Preparation, characterization and their application in CO_2 capture: A review," *Environmental Science and Pollution Research* 31(28), 40008-40062. DOI: 10.1007/s11356-023-28023-9

Socaciu, L. G. (2012). "Thermal energy storage with phase change material," *Leonardo Electronic Journal of Practices and Technologies* 20, 75-98.

Sun, W., Bai, L., Chi, M., Xu, X., Chen, Z., and Yu, K. (2023). "Study on the evolution pattern of the aromatics of lignin during hydrothermal carbonization," *Energies* 16(3), 1089.

Wang, C., Feng, L., Li, W., Zheng, J., Tian, W., and Li, X. (2012). "Shape-stabilized phase change materials based on polyethylene glycol/porous carbon composite: The influence of the pore structure of the carbon materials," *Solar Energy Materials and Solar Cells* 105, 21-26.

Wen, R., Zhang, X., Huang, Z., Fang, M., Liu, Y., Wu, X., Min, X., Gao, W., and Huang, S. (2018). "Preparation and thermal properties of fatty acid/diatomite form-stable composite phase change material for thermal energy storage," *Solar Energy Materials and Solar Cells* 178, 273-279. DOI: 10.1016/j.solmat.2018.01.032

Xu, C., Wang, W., Zhang, H., and Fang, G. (2022). "Thermal properties of lauric acid-palmitic acid eutectics/polyvinyl butyral/carbon nanofibers as shape-stable phase change materials," *Thermochimica Acta* 715, article 179300. DOI: 10.1016/j.tca.2022.179300

Yahya, M. A., Al-Qodah, Z., and Ngah, C. W. Z. (2015). "Agricultural bio-waste materials as potential sustainable precursors used for activated carbon production: A review," *Renewable and Sustainable Energy Reviews* 46, 218-235. DOI: 10.1016/j.rser.2015.02.051

Yang, Z., Deng, Y., and Li, J. (2019). "Preparation of porous carbonized woods impregnated with lauric acid as shape-stable composite phase change materials," *Applied Thermal Engineering* 150, 967-976. DOI: 10.1016/j.applthermaleng.2019.01.063

Yuan, Y., Li, T., Zhang, N., Cao, X., and Yang, X. (2016). "Investigation on thermal properties of capric–palmitic–stearic acid/activated carbon composite phase change materials for high-temperature cooling application," *Journal of Thermal Analysis and Calorimetry* 124(2), 881-888. DOI: 10.1007/s10973-015-5173-0

Zhang, P., Hu, Y., Song, L., Lu, H., Wang, J., and Liu, Q. (2009). "Synergistic effect of iron and intumescent flame retardant on shape-stabilized phase change material," *Thermochimica Acta* 487(1), 74-79. DOI: 10.1016/j.tca.2009.01.006

Article submitted: March 8, 2025; Peer review completed: May 17, 2025; Revisions accepted: May 29, 2025; Published: June 2, 2025.
DOI: 10.15376/biores.20.3.5914-5931